

The most sensitive type of optical sensors is phase modulation sensors. The phase ϕ is given [1, 2] by:

$$\phi = K n L$$

Where K is the wave propagation constant, L is the optical path (the specimen depth along the geometrical path) and n is the refractive index. Any variation in either n or L results in a phase changes. Mach-Zender interferometer, shown in Figure 1 has been used. This device is used for sensing acoustic signals, pressure, temperature and magnetic field [1,2,3].

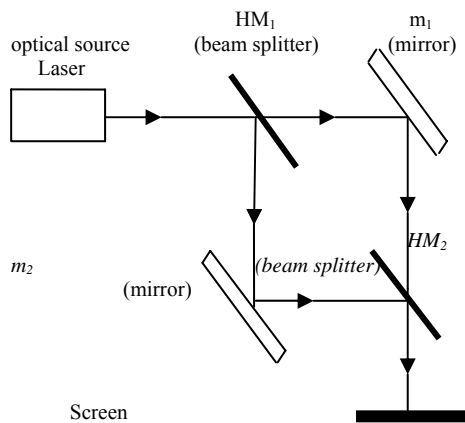


Figure 1: Mach-Zender interferometer configuration [1].

Theory

Phase of light (ϕ) propagating through a material is defined as below.

When specimen is subjected to a modulating effect, an optical phase shift, $\Delta\Phi$, occurs in the light beam, which is given by [4,8].

$$\Phi = K_0 n \Delta L + L K_0 \Delta n$$

$$\Delta\Phi = K_0 n L \epsilon_z + L K_0 \Delta n \text{ ----- (1)}$$

The first term is the change in the length effect and can be given in terms of the axial strain ϵ_z . The second term is the change in the refractive index and is computed from the strain – optic effect which is given by the change in the optical indicatrix [4];

$$\Delta \left[\frac{1}{n^2} \right]_i = \sum_{j=1}^6 P_{ij} \epsilon_j \text{ (2)}$$

Where the P_{ij} , is the optical constant (Pockel's constant).

When a material is under isotropic stress with no shear strain then:

$$\epsilon_4 = \epsilon_5 = \epsilon_6 = 0$$

Only $i,j=1,2,3$, elements of strain-optic tensor for homogeneous isotropic material are needed to be considered where $P_{11}=P_{22}=P_{33}$, $P_{12}=P_{21}=P_{13}=P_{31}=P_{23}=P_{32}$ [4]; Therefore, the change in the optical indicatrix may be expressed as:

$$\Delta \left[\frac{1}{n^2} \right]_{x,y,z} = P_{11} \epsilon_x + P_{12} \epsilon_y + P_{12} \epsilon_z \text{ (3)}$$

The relative variation of the refractive index due to the photoelastic effect can be expressed as [4]:

$$\Delta n = - \frac{n^3}{2} \Delta \left[\frac{1}{n^2} \right]_{x,y,z} \text{ (4)}$$

On substituting eq.(3) in eq. (4), takes the form,

$$\Delta n = - \frac{n^3}{2} (P_{11} \epsilon_x + P_{12} \epsilon_y + P_{12} \epsilon_z) \text{ (5)}$$

Thus on substituting eq. (5) into eq. (1), an expression for $\Delta\Phi$ is obtained as[5,6,7].

$$\Delta\Phi = \left[\frac{-K_0 n(1-\mu)}{E} + \frac{K_0 n^3}{2E} (1-2\mu)(P_{11} + 2P_{12}) \right] PL \text{ ... (6)}$$

Where μ is the Poisson's ratio, E is the Young's modulus and

$$P_{11} + 2P_{12} = ((e-1)(e+2))/e^2$$

e is the dielectric constant of the material used in sensors which is related to the refractive index by $e = n^2$.

Equation 6 explains the relation between the optical phase shift and pressure. It is used in the present work to calculate the theoretical results. This type of modulation is the most sensitive type. Phase shifts as small as 10^{-7} rad may be detected for a wavelength of 0.83 μm [1,2].

Experimental Method

The experimental setup is presented in Figure 2. Before placing the specimen, the interference pattern must be observed.

The overlapping of the two beams must be observed on the screen. Then the two overlapping beams interfere to form a series of circularly bright and dark fringes.

The specimen confined between the two plates of the loading system, is placed in one of paths. The correcting sheets (which act as a reference specimen) is placed in the other path.

The specimen is uniformly and gradually compressed. The change in the phase is observed visually and by a proper electronic detector, monitoring and counting the displacement of the fringes in the interference pattern.

(phase response curve) in three cases exponential. From these curves it can be seen that the linear behavior is common to all of them. This linearity in the behavior is reversible i.e. the behavior is the same in case of the compression and relaxation. But the sensitivity follows almost an oscillating behavior with respect to the length of the samples as shown in

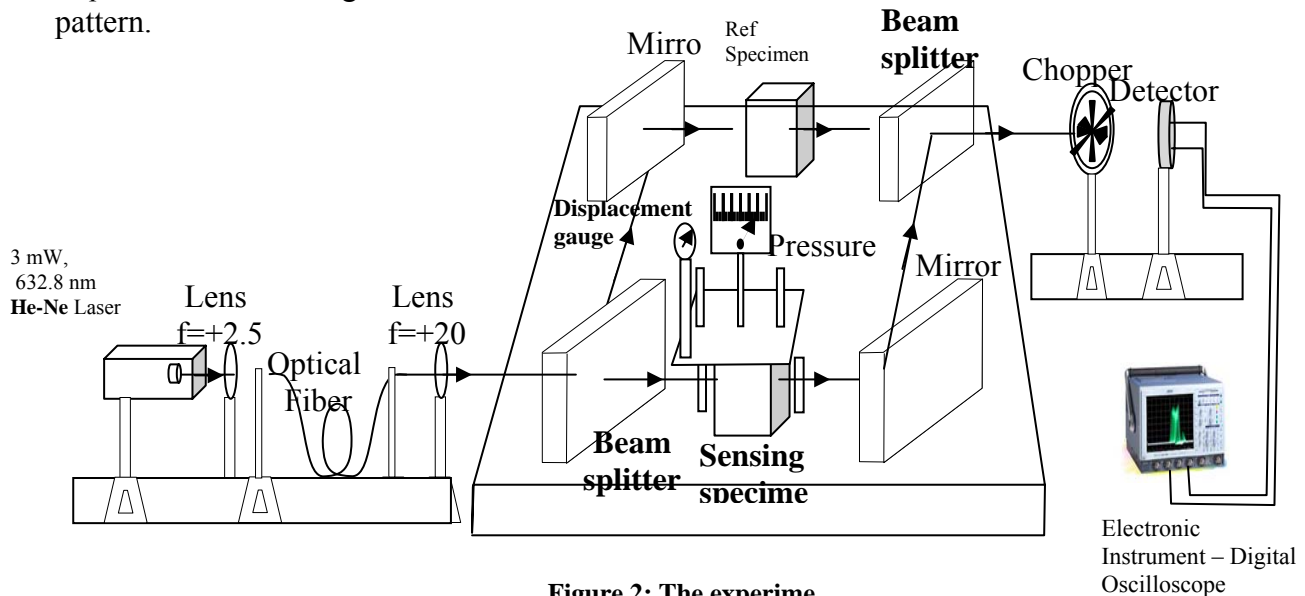


Figure 2: The experimental setup configuration.

In the case of the electronic detector, maximum intensity indicates bright fringes, while a minimum intensity is considered as dark fringe. The numbers of fringes displaced are given by the number of changes in intensity.

One fringe displacement indicates a phase change of π (the displacement from bright to dark indication). The same procedure is repeated for all specimens.

Results and Discussion

Phase Response

Rectangular samples of PMMA are employed to see the effect of the sample dimensions on the phase response. Different geometrical dimensions length, depth and height are considered.

Sample Length Effect

Samples of 6mm in depth and 35mm in height are employed in these experiments.

Fig.3-a and 3-b both show the behavior of the applied pressure to a 14mm, 19mm, 26mm, 30mm, 34mm, 40mm, 43mm, 52mm and 86mm length samples as a function of the number of fringes representing the variation in phase

Figure 4. This may be explained as due to the rotation of the chain of the polymer material. As the chain is rotated, the light will be incident at different configuration of the molecules (i.e. different faces of the chain). As the length increases the sample becomes more susceptible to the pressure to certain limit at which the chain is rerouted to its almost original orientation, where it starts the cycle once again. Nevertheless as apart of the oscillating behavior, the sensitivity decreases with increasing the length.

Sample Depth Effect

Three samples of 35mm in height and 14 mm, 26 mm, 52 mm in length are employed in this test. The depths of the samples are 6 mm, 24 mm and 41mm as shown in figures 3,5a, 5b. Figure 6 shows the behavior of the sensitivity as a function of the depth of the sample. The sensitivity seems to be first decreasing very rapidly and then level off.

Sample Height Effect

Two samples of 6 mm in depth and 26 mm, 52mm ,86 mm in length are considered. The height of two samples are 15mm and 35mm.Figs.(3)and (7)show the phase response curve for these samples. The sensitivity of the 15mm height sample is higher than that for the 35mm in height sample.

Conclusion

The data obtained show that a pressure sensor may be designed based on the interference output of a laser light beam passing through a PMMA specimen.

A flexible and safe transmission medium for the modified signal is possible using optical fibers. The results show that a variable dynamic range and resolution of the pressure may be achieved using different dimensions of the sensing specimen.

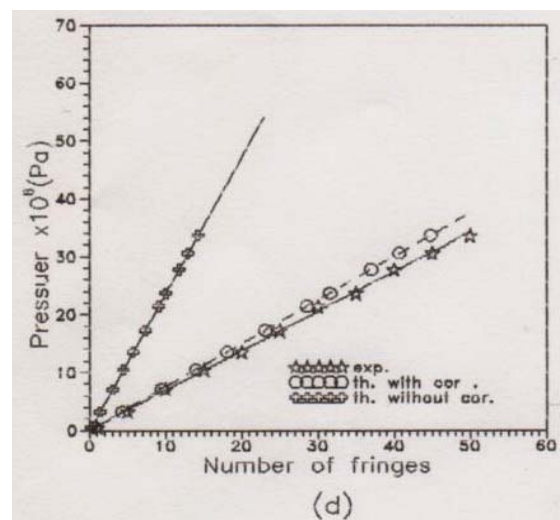
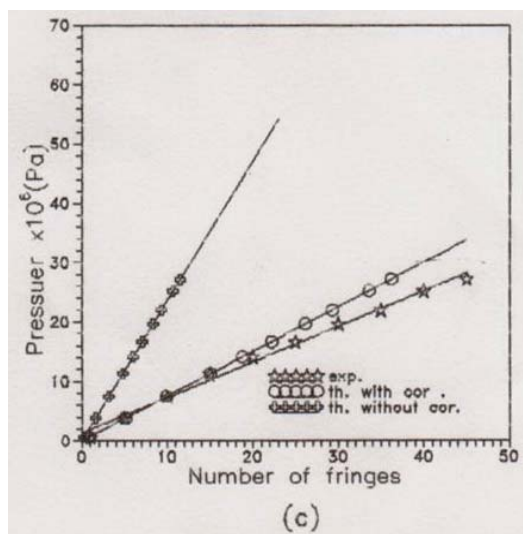
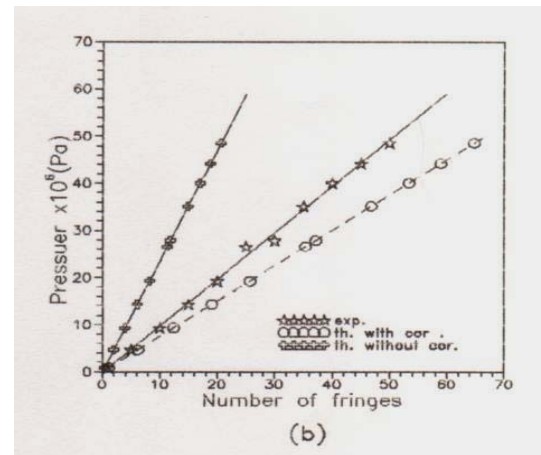
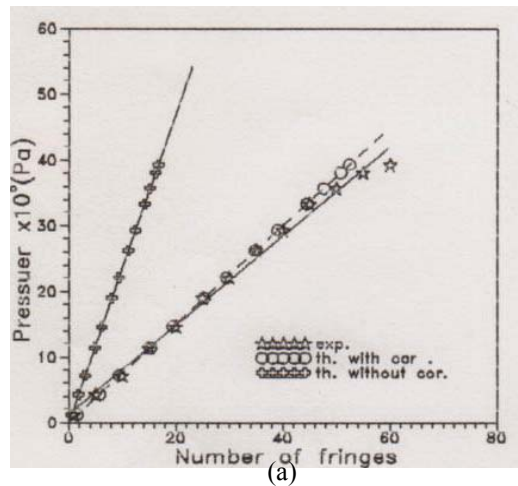


Figure 3-a: Theoretical, experimental and corrected theoretical phase response curve for the (6mm) in depth and 35mm in high samples with length (a) 14mm (b) 19mm (c) 26mm (d) 30mm.

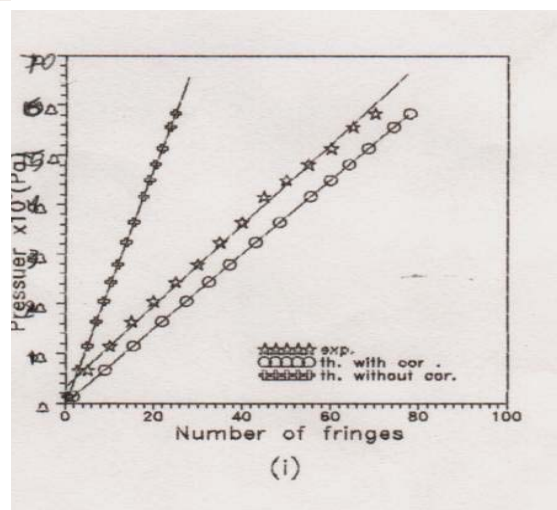
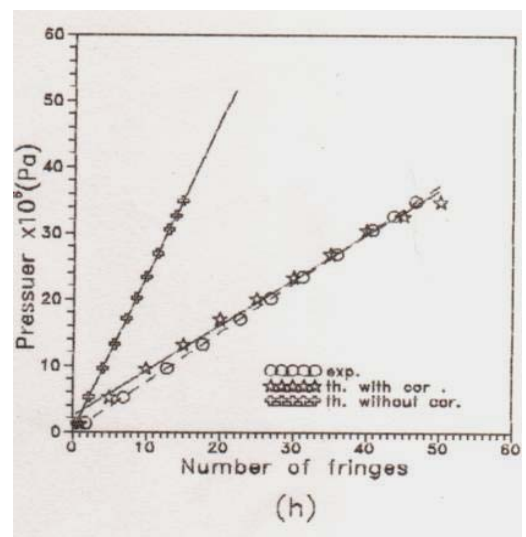
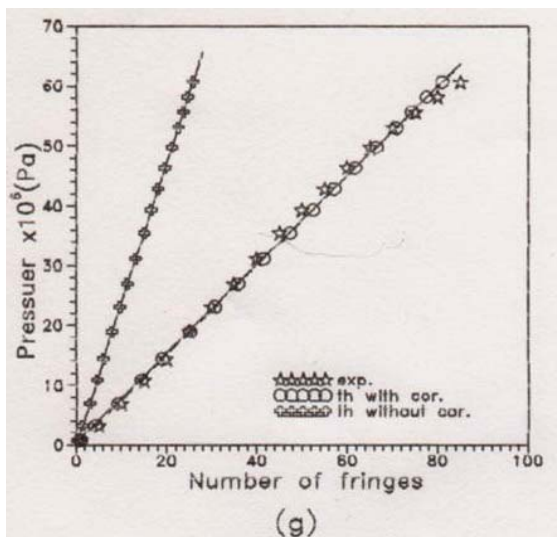
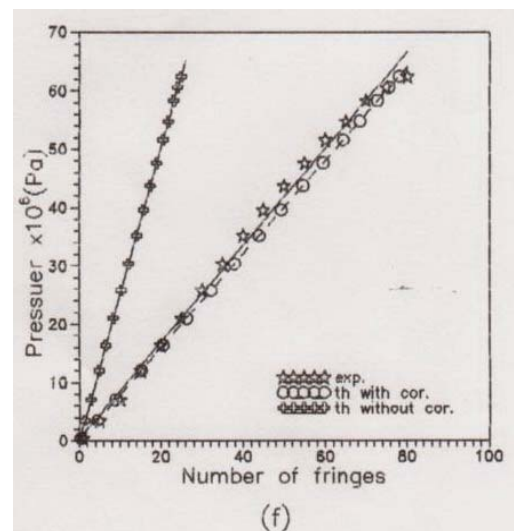
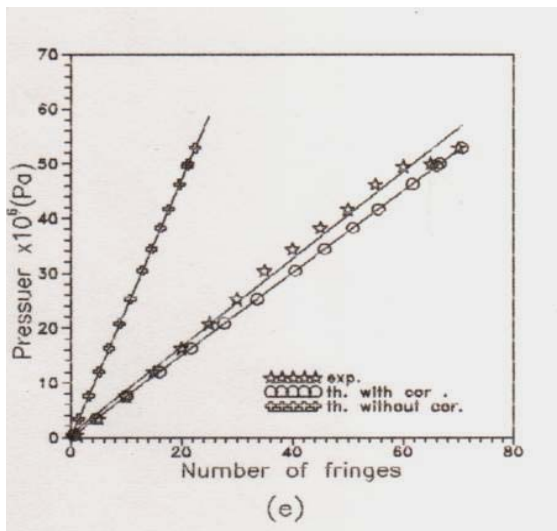


Figure 3-b: Theoretical, experimental and corrected theoretical phase response curve for the (6mm) in depth and (35mm) in height samples with length (e) 34mm (f) 40mm (g) 43mm (h) 52mm (i) 86mm

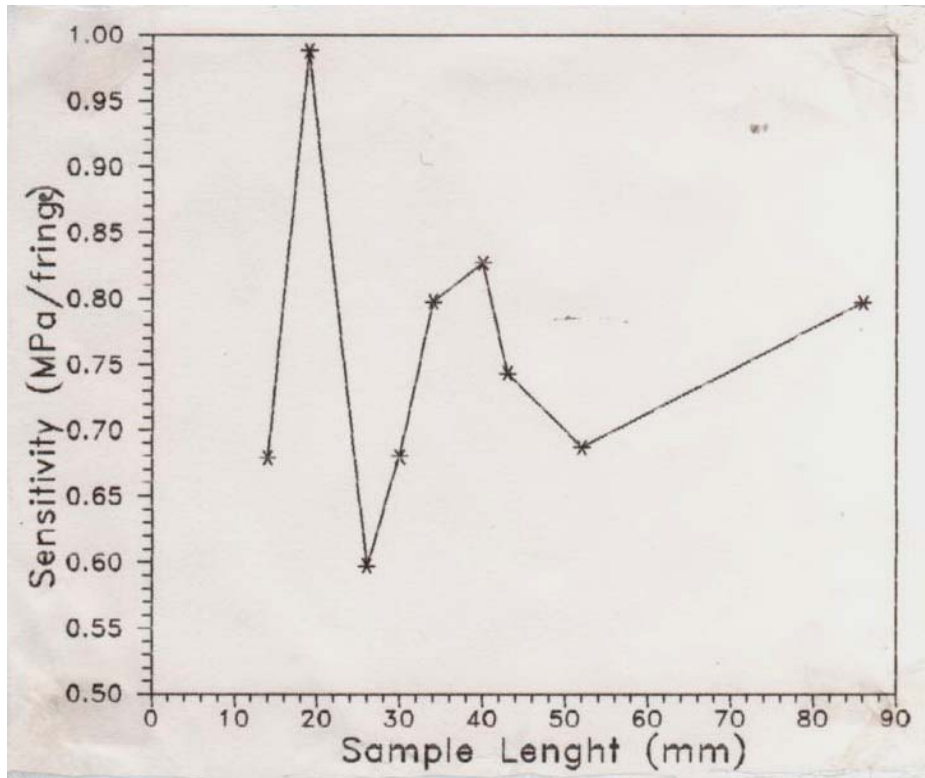


Figure 4: Phase sensitivity of 6mm in depth 35mm height samples as a function of samples length.

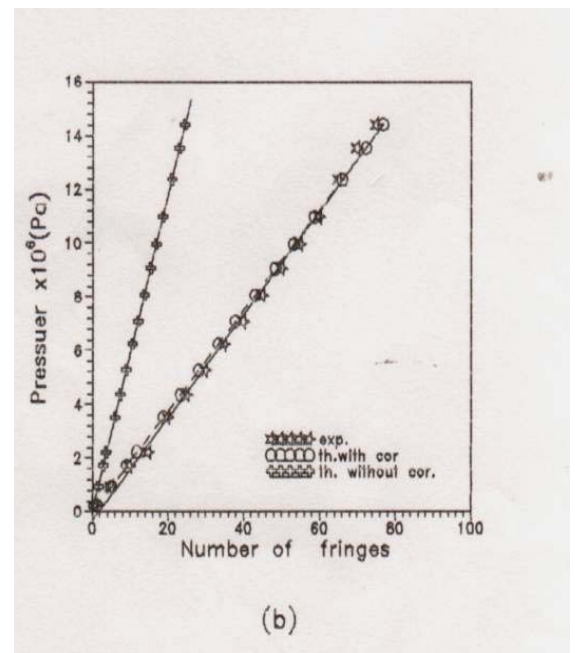
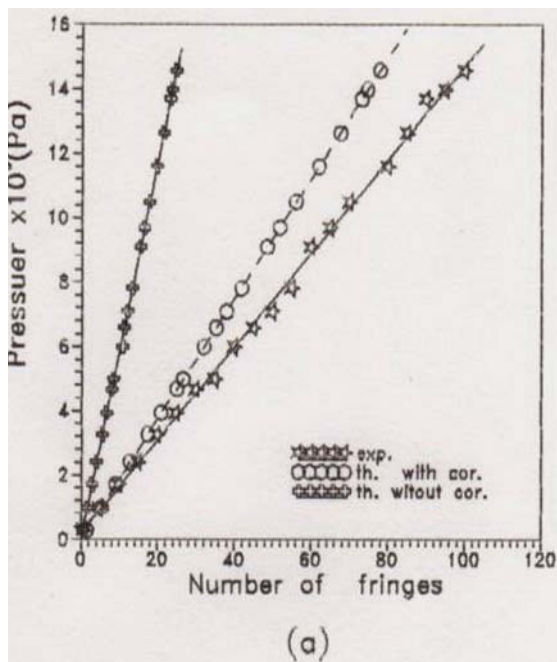


Figure 5-a: Theoretical, experimental and corrected theoretical phase response curve for the 24mm in depth and 35mm in height samples with length (a) 14mm (b) 52mm.

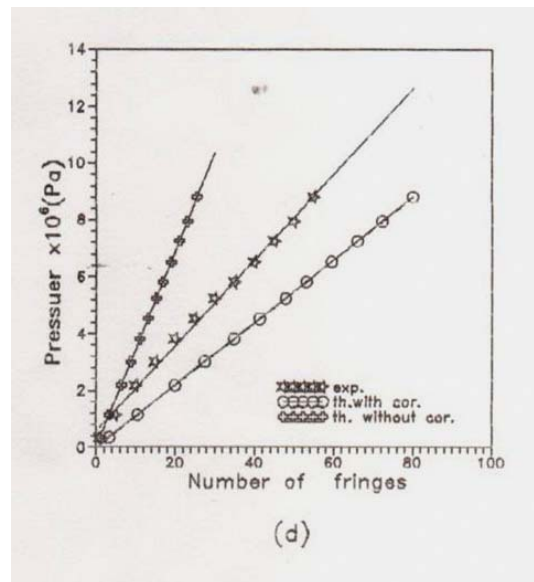
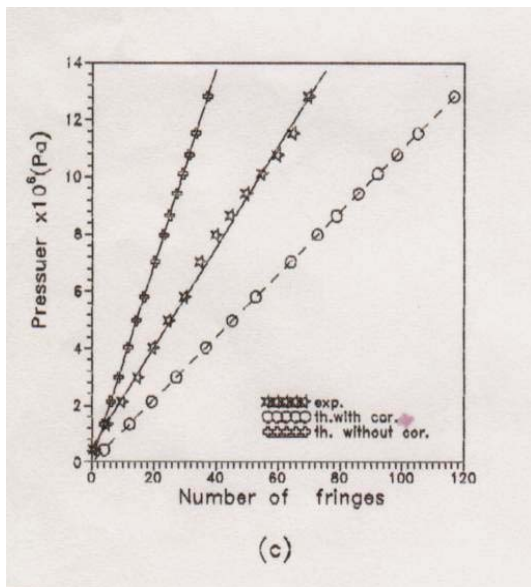
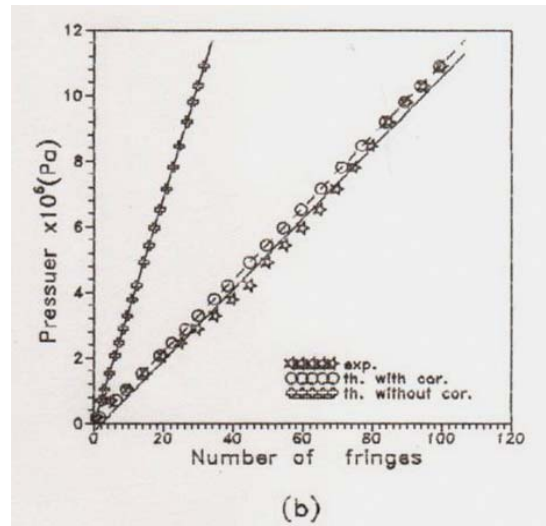
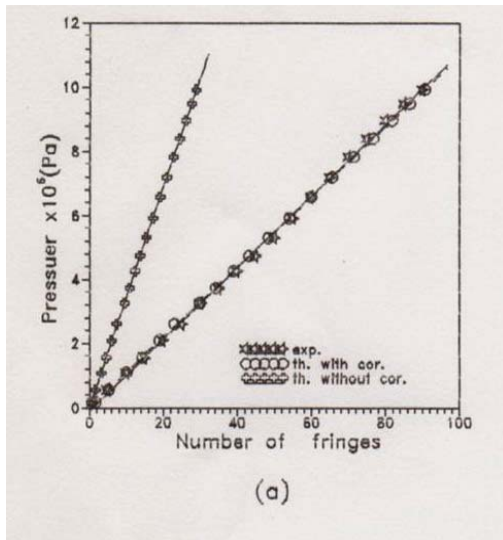


Figure 5-b: Theoretical, experimental and corrected theoretical phase response curve for the 41mm in depth and 35mm in height samples with length (a) 14mm (b) 26mm (c) 52mm (d) 86mm.

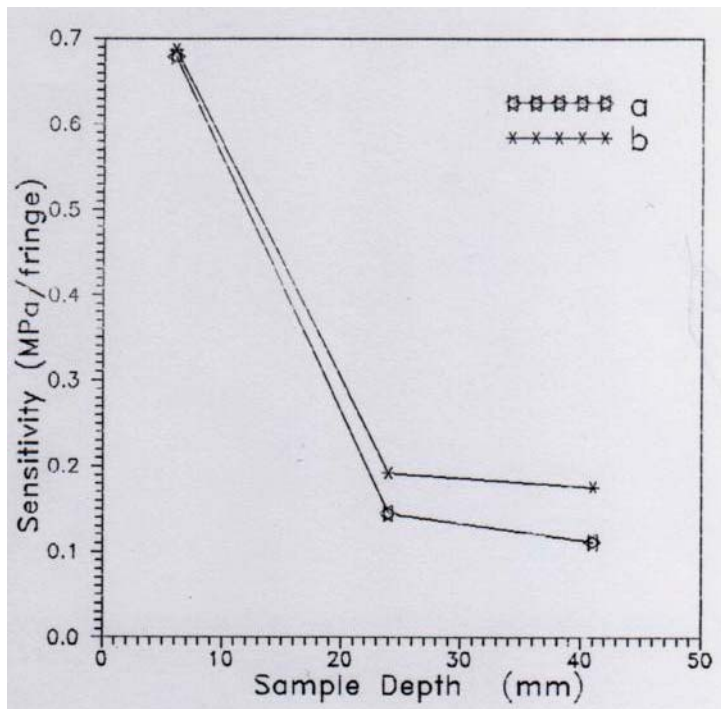


Figure 6: Phase sensitivity for the samples with (35mm) in height and width length (a) 14mm (b) 52mm as a function of samples depths.

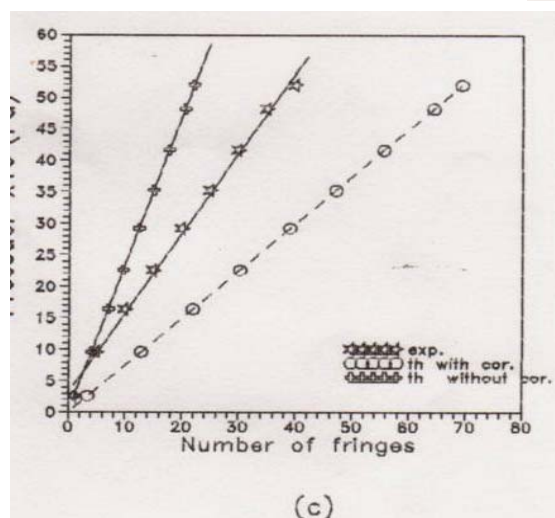
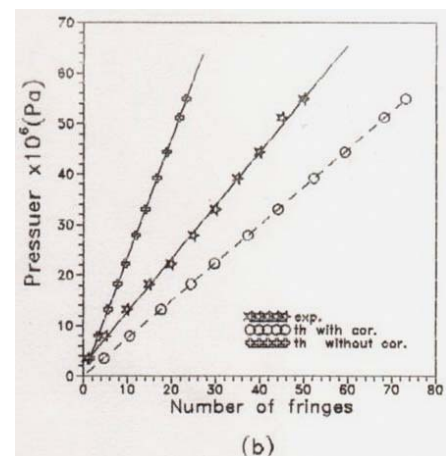
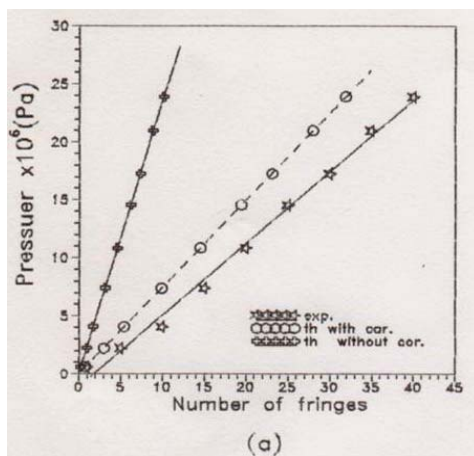


Figure 7: Theoretical, experimental and corrected theoretical phase response curve for the (6mm) in depth and (15mm) in height samples with length (a) 26mm (b) 52mm (c) 86mm.

References

1. Giallorenzi, T., J. Bucaro, G. Sigel and R. Priest. **1984**. Optical Fiber Sensor Technology, IEEE *J. Quantum Electronics*, **18**(4):626-667.
2. Davis C. **1983**. Fiber Optic Sensor , *SPIE*, **412**(0-7), P2,
3. Hocker, G. **1979**. Fiber Optic Sensing of Pressure and Temperature, *Applied Optic*,**18**(9):1445.
4. Saprud, J. **1979**. Acousto-Optics, New York: Wiley– Interscience Publication.
5. Gianino P. and B. Bendow, **1981**. Calculations of Stress –Induced Change in the Transverse Refractive –Index Profile of Optical Fibers, *Applied Optics* **20**(3):430.
6. Timoshenko, S. and J. Goodier, **1951**. Theory of Elasticity, New York: McGraw-Hill , INC.
7. Hajim, K. R. Yoysif and K. Naimc, **1990**. the Optomechanical Properties of PMMA and their Use as a Pressure Sensor , Part I *SPIE* .
8. Miao Yu. **2008**. Fiber Optics Sensor Technology" IMAC XXVI,Orlando,FL.
9. Subir Kumar Sarkar **2009**. Optical Fibers and Fiber Optics Communication systems. S. Chand and company Ltd.